Buoyant Convection Driven by an Encapsuled Spinning Disk with Axial Suction

Jae Min Hyun* and Jae Won Kim†
Korea Advanced Institute of Science and Technology, Seoul, Korea

An analysis is made of the flow and thermal structures of a viscous fluid confined in a vertically mounted cylindrical container. The bottom endwall disk and the sidewall are rotating steadily about the cylinder axis, and the top endwall disk is stationary. A gravitationally stable temperature difference is applied on the container boundaries. In order to formulate a flow model of greater relevance to the Czochralski growth of crystals from melt, an axial suction through the rotating disk and a concomitant radial inflow through the sidewall are imposed. The main motivation of the study is to examine the effects of suction in a finite configuration and of the fluid stratification. Numerical solutions to the axisymmetric Navier-Stokes equations with the Boussinesq assumption have been obtained. The parameter ranges are that the rotational Reynolds number is large and the cylindrical aspect ratio, the Prandtl number, the suction parameter, and the stratification number are all of order unity. Comprehensive flow details have been acquired. For a stratified flow, the principal balance in the interior core is characterized by a relationship between the radial temperature gradient and the vertical shear in the azimuthal flow. The magnitudes of azimuthal flows in the core region increase as the suction increases. Significant differences are seen in the meridional flow patterns as the effects of suction and stratification are incorporated in the analysis. As the stratification effect becomes appreciable, larger portions of the meridional fluid transport are short-circuited directly from the sidewall to the rotating disk. The structure of the thermal field for a stratified fluid is plotted to illustrate the dominant modes of heat transfer. It is shown that the convective heat transfer associated with the meridional fluid transport is dominant in the main body of the flowfield.

Introduction

THE flow of an incompressible viscous fluid inside a finite cylinder when one of its endwall disks is spinning has been extensively investigated recently.[1-8] This internal flow serves as a classical model, exhibiting the dynamic ingredients intrinsic to rotating fluid systems. Also, the flows confined between two parallel coaxial disks, one rotating and the other stationary, are of great relevance to a host of technological applications, i.e., fluid machinery, chemical mixers, centrifuges, computer disk drive systems, and lubrication systems, to name a few. For a definitive problem formulation, we shall envision that the cylinder axis is aligned vertically and the spinning disk forms the bottom endwall of the cylinder.

As for usual engineering applications, we shall be concerned with the situations in which the rotational Reynolds number Re is large. Here, Re is defined as $Re = \Omega h^2/\nu$, where Ω is the angular frequency of the rotating disk, h the axial separation of the two disks, and ν the kinematic viscosity of the fluid. It has been established that when $Re \gg 1$, one principal dynamic component is the Ekman layers that form on the endwall disks perpendicular to the rotation axis. Owing to the fluid pumping mechanism by the Ekman layers, a small axial flow is induced; this in turn gives rise to the secondary flows in the meridional plane.

The modification in the flow brought about by imposing a uniform axial suction through the rotating disk at large Reynolds numbers was examined by Wilson and Schryer[9] (hereafter referred to as W&S). This is an important issue, since it is basically the axial flow induced by the Ekman layers that profoundly influences the global flow structure in the meridional plane. The introduction of a forced axial outflow through the rotating disk interferes with the Ekman layer-induced meridional circulation; consequently, the azimuthal velocity field in the core is significantly affected.

The motivations behind the numerical studies conducted by W&S were to delineate the salient features of the fluid dynamical aspects of the melt motions in a rotating crucible; these are crucial elements in the crystal growth. Specifically, attention is focused on the currently popular Czochralski method of growing crystals from the melt (Wilson,[10,11] Ostrach[12]). For those processes, the rotational Reynolds number is large, typically in the order of $O(10^4) \sim O(10^6)$ (see Ostrach,[12,14] Langlois[13]). The imposition of a uniform axial suction through the rotating disk models the rotating crystal rod, which is pulled out slowly in the axial direction (Wilson[10,11]). It is well known that the axial velocity induced by the Ekman layer pumping, W_E, is $O(Re^{-1/2}\Omega h)$. The investigations by W&S dealt with the cases when the imposed uniform axial suction velocity W_s was comparable with W_E. Consequently, they expressed W_s as $W_s = -SRe^{-1/2}\Omega h$, where S was the suction parameter, which was assumed to be $O(1)$. In passing, we note that the Ekman number $E\ [\equiv 1/Re]$ is often used in the literature. In the present paper, however, in line with W&S, we shall employ the rotational Reynolds number.

The numerical procedures adopted by W&S were to compute the flow confined between two parallel infinite disks, one rotating and the other stationary. This assumption of an infinite disk configuration reduced the governing partial differential equations to a set of coupled ordinary differential equations, which were readily amenable to numerical integration. The infinite-disk solutions revealed that as the suction increased, the rotation rate in the core increased. Under a sufficiently strong suction, the core rotation rate exceeded that of the spinning disk, and the Ekman layer reappeared on both disks, but the direction of the radial flow in the Ekman layer near the spinning disk was reversed. These numerical results were useful in depicting the qualitative character of the flow when axial suction was applied through the rotating disk.

In order to pursue a proper understanding of more realistic flows that occur in the Czochralski growth of crystals, however, the original model of W&S has to be extended in two important areas. First, as was remarked by W&S, a serious

Received Jan. 15, 1988; revision received May 2, 1988.

*Professor, Department of Mechanical Engineering.
†Graduate Student, Department of Mechanical Engineering.

question arises as to whether the highly idealized infinite-disk solutions provide an adequate description of the real flows in finite geometry. The recent account by Hyun and Kim[15] (hereafter referred to as H&K) proposed a finite-cylinder flow analogy to the infinite-disk model of W&S. In the model of H&K, as the axial suction was applied at the rotating disk, the uniformly distributed replacement fluid was admitted radially inward through the corotating cylindrical sidewall. The azimuthal flow structure in finite configuration was shown to be consistent with the predictions of the infinite disk model in the central region away from the sidewall. Due to the sidewall effect, however, the finite-geometry analogy displayed significant radial variations in both the azimuthal flow and the meridional fluid transport. Secondly, if the results of any flow model are to be of value to assessing the melt motions in realistic crystal growth situations, the effect of fluid stratification must be incorporated in the analysis. In the Czochralski growth or in other techniques of growing crystals from the melt, the melt is highly stratified due to the differential heating along the solid boundaries (Wilson,[10,11] Kamotani and Ostrach[16]). The effect of fluid stratification is an essential factor in determining the basic properties of the flow confined in a rotating frame (e.g., Pedlosky[17]). A stable stratification in the fluid system is anticipated to suppress the vertical motions. Accordingly, both the Ekman layer-induced axial flows and the externally forced outflow through the spinning disk will be affected by the presence of the fluid stratification. The consequences will be distinctly different from those for a homogeneous fluid.

The extension of the model of W&S, as proposed in the present study, entails potentially significant implications for the advancement of crystal growth methodologies. The possible utilization of the reduced-gravity space environment warrants an in-depth analysis of the buoyancy effects in a confined fluid system. In particular, knowledge of the gravity-induced buoyant convection in the Earthbound laboratory is needed to identify the extents of feasible exploitation of the extraterrestrial environment to grow crystals from melts.

In this paper, in an effort to achieve a flow model of greater relevance to the practical crystal growth process, we shall describe how the flow in finite configuration, driven by a rotating disk with an axial suction applied through it, is influenced by the inclusion of the stratification effect. This will represent an improved version of the original model of W&S, addressing the aforementioned two areas of extension, namely, the effects of finite geometry and fluid stratification. We have sought numerical solutions to the axisymmetric Navier-Stokes equations in finite geometry, making use of the Boussinesq assumption. Comprehensive and systematic flow data have been acquired to illustrate the flow and thermal structures. Results are presented over the ranges of the suction parameter $S \sim O(1)$ and the stratification parameter $B \sim O(1)$, where $B \equiv (N/\Omega)^2$, N being the system buoyancy frequency.

The Model

The governing equations are the axisymmetric incompressible Navier-Stokes equations with the Boussinesq fluid assumption. Written for cylindrical coordinates (r,θ,z) with respective velocity components (u,v,w), these are

$$\frac{\partial u}{\partial t} = -\frac{1}{r}\frac{\partial}{\partial r}(ru^2) - \frac{\partial}{\partial z}(uw) - \frac{1}{\rho_b}\frac{\partial p}{\partial r} + \frac{\bar{v}^2}{r} + \nu(\nabla^2 u - \frac{u}{r^2}) \quad (1)$$

$$\frac{\partial \bar{v}}{\partial t} = -\frac{1}{r}\frac{\partial}{\partial r}(ru\bar{v}) - \frac{\partial}{\partial z}(\bar{v}w) - \frac{u\bar{v}}{r} + \nu(\nabla^2 \bar{v} - \frac{\bar{v}}{r^2}) \quad (2)$$

$$\frac{\partial w}{\partial t} = -\frac{1}{r}\frac{\partial}{\partial r}(ruw) - \frac{\partial}{\partial z}(w^2) - \frac{1}{\rho_b}\frac{\partial p}{\partial z} + \alpha g T + \nu\nabla^2 w \quad (3)$$

$$\frac{\partial T}{\partial t} = -\frac{1}{r}\frac{\partial}{\partial r}(ruT) - \frac{\partial}{\partial z}(wT) + \kappa\nabla^2 T \quad (4)$$

$$\frac{1}{r}\frac{\partial}{\partial r}(ru) + \frac{\partial w}{\partial z} = 0 \quad (5)$$

where $\nabla^2 = (1/r)(\partial/\partial r)(r\partial/\partial r) + \partial^2/\partial z^2$, $\bar{v}$ is the azimuthal velocity relative to the rotating coordinate, i.e., $v = \bar{v} + r\Omega$, p the reduced pressure, T is the temperature such that the full temperature equals $T_b + T$, and the equation of state is

$$\rho = \rho_b(1 - \alpha T) \quad (6)$$

in which T_b and ρ_b are the reference values of temperature and density, respectively.

Consider a vertically mounted right circular cylinder of radius a and height h filled with a fluid having kinematic viscosity ν, thermal diffusivity κ, and coefficient of volumetric expansion α. These physical properties are taken to be constant. The fluid stratification is produced by maintaining a temperature differential ΔT between the top and bottom endwall disks, the top being hotter than the bottom. The temperature at the sidewall varies linearly between the bottom and top endwalls. The bottom endwall disk and the sidewall rotate steadily about the central axis at angular frequency Ω.

The actual computational procedures were as follows. After the interior fluid had been sufficiently spun up by the action of the rotating bottom endwall disk and the sidewall, the axial suction through the rotating bottom disk, measured by $W = W_s$, and the concurrent radial inflow through the sidewall were applied. In summary, the boundary conditions can be expressed as

$$u = 0, \quad v = r\Omega, \quad w = W_s, \quad T = 0 \text{ at } z = 0 \quad \text{(the bottom endwall disk)} \quad (7)$$

$$u = v = w = 0, \quad T = \Delta T \text{ at } z = h \quad \text{(the top endwall disk)} \quad (8)$$

$$u = (a/2h)W_s, \quad v = a\Omega, \quad w = 0, \quad T = (z/h)\Delta T \text{ at } r = a \quad \text{(the sidewall)} \quad (9)$$

Evidently, the principal nondimensional parameters are the Reynolds number $Re = \Omega h^2/\nu$; the aspect ratio $A = h/a$; the Prandtl number $Pr = \nu/\kappa$; the suction parameter S, which designates the strength of suction at the rotating disk [$W_s = -SRe^{-1/2}\Omega h$ in Eq. (7)]; and the stratification number $B = (N/\Omega)^2$, where $N = (\alpha g \Delta T/h)^{1/2}$ is the Brunt-Väisälä frequency representing the overall thermal stratification in the fluid system. The proper form of the nondimensionalization scheme that produces these dimensionless numbers may be found in many texts (see e.g., Pedlosky[17]). The problem under the present study is characterized by the parameter orderings $Re \gg 1$; $A,Pr,S,B \sim O(1)$.

The time-marching integration continued until an approximate steady state was attained. The spin-up time scale, $\tau = Re^{1/2}\Omega^{-1}$, gauged the lapse of time for global adjustment in unsteady rotating flows (e.g., Hyun et al.[18]). For convenience, the approximate steady state in the present work was arbitrarily taken to be the state when the flow variables at $r/a = 0.5$, $z/h = 0.5$, changed less than 0.1% over the time interval 0.1τ.

The finite-difference methods developed by Warn-Varnas et al. were amended to solve the system of equations. This method has been shown to provide accurate and reliable numerical solutions to a large class of rotating and stratified fluid flows (e.g., Hyun et al.[18] and Warn-Varnas et al.[19]). This model used the primitive variables on a staggered nonuniform mesh. The pressure was found from a Poisson equation, which was solved by an ADI iterative approach. The specifics of the numerical techniques adopted, including the finite-differencing scheme, were elaborated in Warn-Varnas et al.[19]

Results and Discussion

Several sets of numerical computations were conducted to render comprehensive flow details. For all the calculations performed, $Re = 2.29 \times 10^3$, $A = 1.0$, and $Pr = 6.37$. These values are comparable to those used in the analysis by W&S. In line

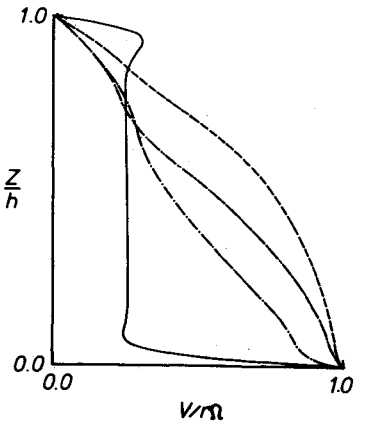

Fig. 1 Axial variation of the angular velocities under no suction ($S = 0.0$). The radial position is at $r/a = 0.5$. ——, $B = 0.0$; —.—, $B = 1.0$; —..—, $B = 2.0$; – – – –, $B = 4.0$.

with the stated objectives of the present study, the values of S and B were varied to scrutinize the effects of the suction in finite geometry and of stratification. In the ensuing discussion, only the exemplary and physically illuminating results will be presented.

Figure 1 displays the axial profiles of the angular velocity $v/r\Omega$ in the regions far away from the sidewall under no suction ($S = 0.0$). For a homogeneous fluid ($B = 0.0$), the azimuthal velocity in the interior core is substantially uniform in the axial direction, which is embodied in the celebrated phenomenon enunciated by the Taylor-Proudman theorem. In the limit of $Re \to \infty$, the classical infinite-disk analysis has demonstrated that $v/r\Omega$ in the core is approximately 0.31 (see Batchelor[20]). The Ekman layers form on both disks, which adjust the core solution to the boundary conditions at the disks. The introduction of a stable stratification brings about qualitative changes in the primary flowfield. First, the inhibition of the vertical motions leads to the weakening of the Ekman layers. Second, in the interior core, the axial uniformity of the azimuthal velocities is no longer sustained. As the stratification effect increases, the azimuthal velocity field in the bulk of the flow domain entails vertical velocity shear. This can be readily seen in the equation of vorticity, $\eta[\equiv (\partial u/\partial z) - (\partial w/\partial r)]$, which may be obtained by cross-differentiating Eqs. (1) and (3):

$$\frac{\partial \eta}{\partial t} = -u\left(\frac{\partial \eta}{\partial r} - \frac{\eta}{r}\right) - w\frac{\partial \eta}{\partial z} + 2\frac{\bar{v}}{r}\frac{\partial \bar{v}}{\partial z} + 2\Omega\frac{\partial \bar{v}}{\partial z} + \nu\left[\frac{\partial}{\partial r}\left(\frac{1}{r}\frac{\partial}{\partial r}r\eta\right) + \frac{\partial^2 \eta}{\partial z^2}\right] - \alpha g\frac{\partial T}{\partial r} \tag{10}$$

As stated previously, the numerical results of velocity and temperature were obtained by solving the full nonlinear Navier-Stokes equations. By introducing these numerical data into Eq. (10), we evaluated the magnitude of each term in the equation. Such a diagnostic analysis yielded that, in the inviscid core, the dominant balance was

$$\alpha g\frac{\partial T}{\partial r} \cong 2\Omega\frac{\partial \bar{v}}{\partial z}$$

This is the well-known thermal wind relation (e.g., Pedlosky[17]). Also, as the Ekman layers fade in strength, the interior velocity itself approaches smoothly the boundary value at the endwall disk. These features have been well documented (e.g., Pedlosky[17]).

Figure 2 illustrates the associated meridional circulation patterns under no suction. In the figures, we plot the meridional stream function ψ, which is defined such that

$$u = -\frac{1}{r}\frac{\partial \psi}{\partial z},\quad w = \frac{1}{r}\frac{\partial \psi}{\partial r}$$

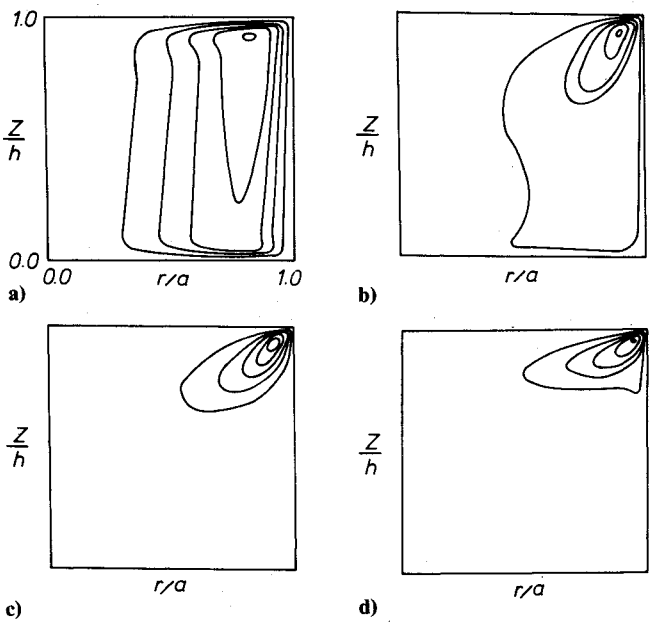

Fig. 2 Plots of the meridional stream function ψ under no suction ($S = 0.0$). Values ψ of are expressed in units of $Re^{-1/2}\Omega h^2 a$, and $\Delta\psi$ denotes the contour increment: a) $B = 0.0$, $\psi_{max} = 0.20$, $\psi_{min} = 0.04$, $\Delta\psi = 0.04$; b) $B = 1.0$, $\psi_{max} = 0.10$, $\psi_{min} = 0.02$, $\Delta\psi = 0.02$; c) $B = 2.0$, $\psi_{max} = 0.06$, $\psi_{min} = 0.01$, $\Delta\psi = 0.01$; and d) $B = 4.0$, $\psi_{max} = 0.04$, $\psi_{min} = 0.008$, $\Delta\psi = 0.008$.

For a homogeneous fluid (see Fig. 2a for $B = 0.0$), the flow in the bulk of the core is predominantly axial, pulled toward the rotating disk. The Ekman layers on both disks are quite distinct; in the layer near the stationary disk, the flow is radially inward, and in the layer near the rotating disk, the flow is radially outward. The vertical boundary layer near the sidewall accommodates the return circuit to close the counterclockwise meridional circulations. On the other hand, as the stratification effect becomes appreciable, the vertical motions are suppressed due to the stable buoyancy. These are discernible by comparing the magnitudes of the values of ψ (see Figs. 2b–2d). Consequently, the meridional circulation tends to be concentrated near the corner region, where the stationary disk abuts the rotating sidewall. As was stated earlier, the Ekman layers diminish in strength over much of the disk radius. Therefore, the azimuthal flows in the bulk of the cylinder vary continuously between the boundary values at the two endwall disks; the azimuthal flows do not experience rapid changes in the Ekman layers, unlike the case of a homogeneous fluid. These essential characteristics of stratified and rotating flows in a closed chamber have been clearly established, mainly in the context of flow models in physical oceanography (see, e.g., Allen[21]).

Figure 3 portrays the azimuthal flow structure far away from the sidewall under a moderate suction ($S = 2.0$). Notice that for a homogeneous fluid ($B = 0.0$), the rotation rate in the core, which is substantially uniform in the axial direction, exceeds that of the rotating disk. This is simply because the fluid came in at a larger radius ($r = a$) and had the angular velocity appropriate to its entry radius. This is in qualitative agreement with the predictions of the infinite-disk model of W&S. As the stratification effect becomes appreciable, the azimuthal flows in the interior core develop vertical velocity shear, in accord with the aforementioned thermal wind relation. It is clear in Fig. 3 that under a moderate suction, the angular velocity in the main body of the flowfield, with the exception of the Ekman layer region near the stationary disk, is larger than that of the rotating disk. In summary, for the cases of a stratified fluid, the maximum of the magnitude of the angular velocity field tends to increase as the suction increases. This general trend is consistent with the predictions based on the infinite-disk model of W&S.

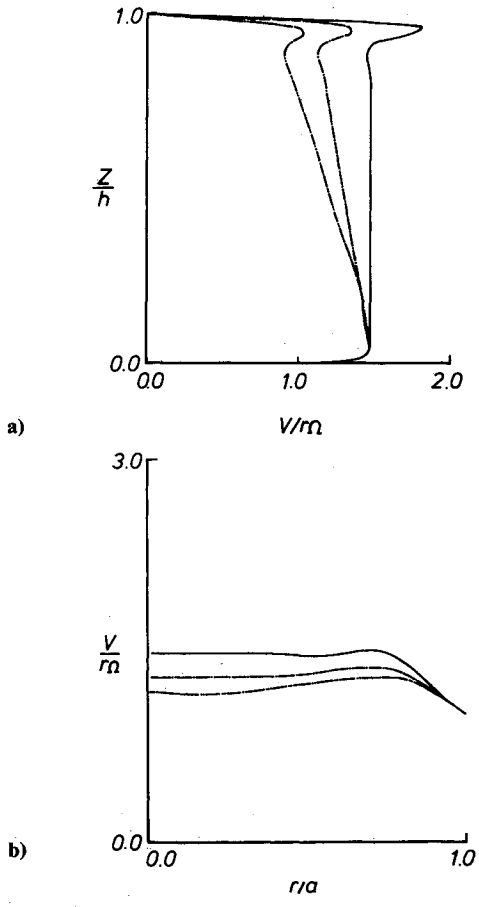

Fig. 3 Profiles of the azimuthal velocity under a moderate suction ($S = 2.0$). a) Azimuthal velocities along $r/a = 0.5$: ——, $B = 0.0$, —·—, $B = 1.0$, —··—, $B = 2.0$; and b) azimuthal velocities along $z/h = 0.5$: ——, $B = 0.0$, —·—, $B = 1.0$, —··—, $B = 2.0$.

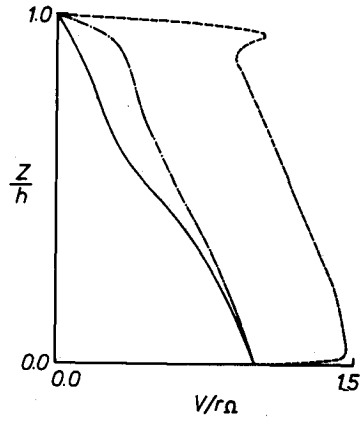

Fig. 4 Axial profiles of the angular velocity of a stratified fluid ($B = 2.0$). The radial position is at $r/a = 0.5$. ——, $S = 0.0$; —·—, $S = 1.0$; – – –, $S = 2.0$.

Figure 4 exemplifies the axial profile of the angular velocity in the interior of a stratified fluid ($B = 2.0$). The trend is clear that as the suction increases, the angular velocity increases; under a sufficiently strong suction, the angular velocity in the bulk of the interior fluid is larger than that of the rotating endwall disk. This feature is qualitatively consistent with the observations elucidated by W&S as well as by H&K for a homogeneous fluid.

The meridional flow patterns under a moderate suction are plotted in Fig. 5. For a homogeneous fluid (see Fig. 5a for $B = 0.0$), as the replacement fluid enters the cylinder uniformly through the sidewall, the principal part of the meridional fluid transport is carried vertically toward the stationary disk via the

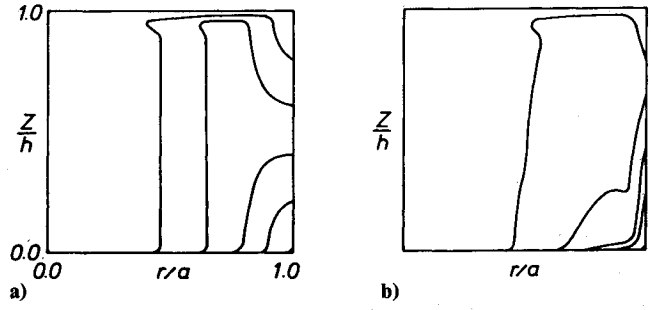

Fig. 5 Same as in Fig. 2, except $S = 2.0$. a) $B = 0.0$, $\psi_{max} = 1.0$, $\psi_{min} = 0.2$, $\Delta\psi = 0.2$; and b) $B = 2.0$, $\psi_{max} = 1.0$, $\psi_{min} = 0.2$, $\Delta\psi = 0.2$.

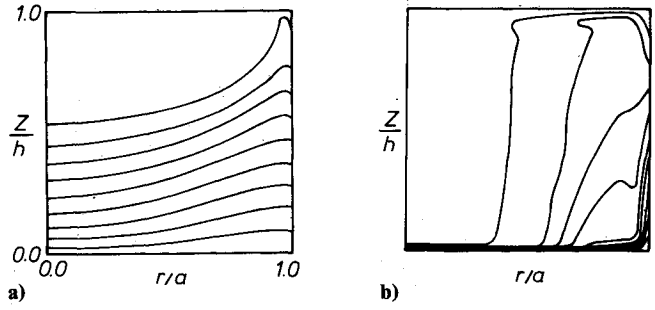

Fig. 6 Plots of the nondimensional temperature $Q = T/\Delta T$ for a stratified fluid ($B = 2.0$). ΔQ denotes the contour increment. a) $S = 0.0$, $\Delta Q = 0.1$; and b) $S = 2.0$, $\Delta Q = 0.1$.

sidewall boundary layer and then radially inward via the boundary layer near the stationary disk. Therefore, in the main body of the cylinder, the meridional flows are substantially axial, and are toward the rotating disk, through which they are discharged outward. Only in a small region near the corner where the sidewall joins the rotating disk, the meridional fluid transport is short-circuited directly from the sidewall to the rotating disk. This pattern of the meridional flows is noticeably altered by the stratification effect (see Fig. 5b for $B = 2.0$). Because of the inhibition of the vertical motions, a larger portion of the meridional fluid transport is short-circuited directly from the sidewall to the rotating disk. The fluid transport that passes through the central region of the cylinder is measurably reduced. This points to an important implication; as the stratification increases, the flow properties that are associated with the replacement fluid entering through the sidewall are not carried far inside into the main body of the flowfield.

Figure 6 shows the isotherm contour maps for the case of a stratified fluid ($B = 2.0$). In a closed cylindrical container with no suction (see Fig. 6a for $S = 0.0$), the thermal field is stratified fairly linearly in the vertical direction in most of the flow domain. However, it is important to note that there exist the radial temperature gradients. These radial temperature gradients, although small in magnitude, tend to be more pronounced in the regions closer to the sidewall. The radial temperature gradients are essential to support the vertical shear of the azimuthal flowfield, as is ascertained in the thermal wind relation of Eq. (10) (see e.g., Pedlosky[17] and Allen[21]). When a moderate suction is applied (see Fig. 6b for $S = 2.0$), the thermal field in much of the cylinder interior is heavily influenced by the meridional fluid transport, and the diffusive effects in the core are insignificant. In the central areas of the meridional plane, large portions of the fluid particles that move toward the spinning disk are those that have originated and/or traveled through the boundary layer near the hot stationary disk. These hot fluid particles are cooled in the vicinity of the rotating disk, the temperature of which is externally controlled at the prescribed value T_b. This creates a narrow zone of intense vertical temperature gradients near the rotating disk in the central region.

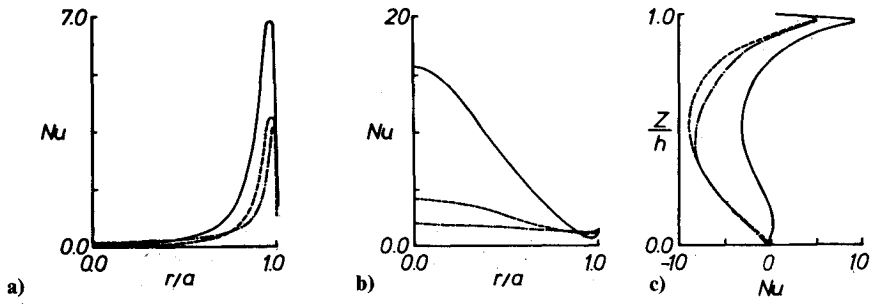

Fig. 7 Variations of the local Nusselt number *Nu* under no suction: ——, $B = 1.0$; ----, $B = 2.0$; — · —, $B = 4.0$. a) *Nu* along the stationary top disk; b) *Nu* along the bottom disk; and c) *Nu* along the sidewall.

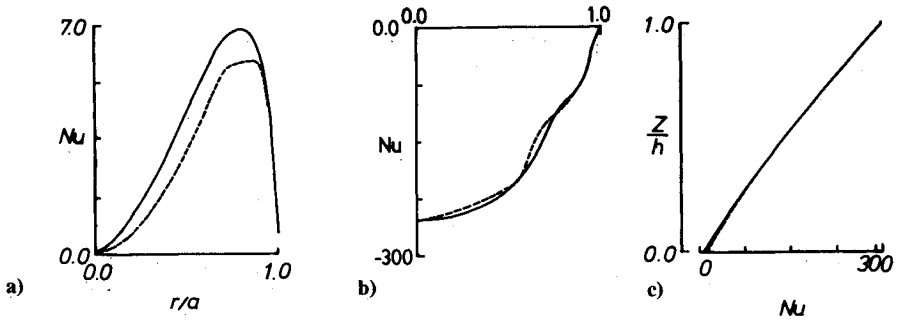

Fig. 8 Variations of the local Nusselt number under moderate suction ($S = 2.0$): a) local Nusselt number on the top disk, ——, $B = 1.0$; ----, $B = 2.0$; b) same as a except for the bottom disk; and c) same as b except for the sidewall.

We now turn to the question of heat transfer along the solid walls. We shall define the local Nusselt number *Nu* as

$$Nu = h\left(k\frac{\partial T}{\partial r} - \rho_b cuT\right)\Big/ k\Delta T$$

along the sidewall $r = a$ and

$$Nu = h\left(-k\frac{\partial T}{\partial z} - \rho_b cwT\right)\Big/ k\Delta T$$

along the endwall disks $z = 0$ and $z = h$. In these expressions, k is thermal conductivity of the fluid and c the specific heat. In the ensuing figures, the Nusselt number will be plotted such that positive values of *Nu* imply the heat transfer toward the fluid inside the cylinder.

Figure 7 shows the local Nusselt number under no suction ($S = 0.0$). In this case, the heat transfer along the solid walls is due entirely to conduction. On the top endwall disk, the isotherms are crowded near the upper right corner, as seen in Fig. 6a; the local heat transfer is intense in this region. On the rotating bottom endwall disk, the vertical temperature gradients are high near the central axis. Over much of the rotating sidewall, the heat transfer in the radial direction is outward from the fluid to the wall.

When a suction is applied, as is exhibited in Fig. 8, the heat transfers along the rotating sidewall and along the bottom endwall disk far outweigh the heat transfer along the stationary top disk (compare the magnitudes of *Nu* in Figs. 8a–c). The heat transfer along the sidewall is dominated by the convective part, and the conductive contribution is minimal. Owing to the predominance of convection, the heat-transfer rate along the sidewall increases almost linearly with height. At the bottom endwall disk, as was pointed out in Fig. 6b, the vertical temperature gradients are very large, especially at small radii. The conductive heat transfer along the stationary top endwall disk make an insignificant contribution to the overall balance of heat transfer. Inspection of Figs. 8a–c clearly demonstrates that a suction of fluid greatly amplifies the global heat-transfer rates because of the enhancement of convective heat transport through the sidewall.

Conclusion

For a homogeneous fluid, the angular velocity in the core is axially uniform and increases as the suction increases. These qualitative features have been captured by the infinite-disk model of W&S. For a stratified fluid, the major balance in the interior is between the effects due to the radial temperature gradient and the vertical shear in the azimuthal flows. The angular velocities are, in general, intensified as the strength of the suction increases.

The meridional flow patterns undergo marked changes as suction and stratification are introduced in the analysis. Of particular interest is the behavior of the meridional fluid transport from the sidewall inflow to the outflow at the rotating disk. Under the effect of stratification, larger portions of the meridional fluid transport are short-circuited directly from the sidewall to the rotating disk.

The structure of the thermal field for a stratified fluid exhibits noticeable radial temperature gradients. They are essential to support the vertical azimuthal velocity shear. When the effect of suction is appreciable, the convective heat transport associated with the meridional fluid transport in the main body of the flowfield is dominant. Consequently, a narrow zone of intense vertical temperature gradients exists near the rotating disk in the central region of the cylinder. The overall heat-transfer balance is dominated by the heat transports carried across the rotating sidewall and the bottom endwall disk.

Acknowledgments

The authors appreciate the constructive comments by the referees. This work was supported in part by a research grant from the Korea Science and Engineering Foundation.

References

[1]Pao, H. P., "A Numerical Computation of a Confined Rotating Flow," *ASME Journal of Applied Mechanics*, Vol. 37, 1970, pp. 480–487.

[2]Tomlan, P. F. and Hudson, J. L., "Flow Near an Enclosed Rotating Disk: Analysis," *Chemical Engineering Science*, Vol. 42, 1971, pp. 1591–1600.

[3]Lugt, H. J. and Haussling, H. J., "Development of Flow Circulation in a Rotating Tank," *Acta Mechanica*, Vol. 18, 1973, pp. 255–272.

[4]Alonso, C. V., "Steady Laminar Flow in a Stationary Tank with a Spinning Bottom," *ASME Journal of Applied Mechanics*, Vol. 42, 1975, pp. 771–776.

[5]Bertela, M. and Gori, F., "Laminar Flow in a Cylindrical Container with a Rotating Cover," *ASME Journal of Fluids Engineering*, Vol. 104, 1982, pp. 31–39.

[6]Dijkstra, D. and Van Heijst, G. J. F., "The Flow Between Two Finite Rotating Disks Enclosed by a Cylinder," *Journal of Fluid Mechanics*, Vol. 128, 1983, pp. 123–154.

[7]Hyun, J. M., "Flow Driven by a Finite, Shrouded Spinning Disk

with Suction," *ASME Journal of Applied Mechanics*, Vol. 52, 1985, pp. 766–770.

[8]Hyun, J. M., "Flow in an Open Tank with a Free Surface Driven by the Spinning Bottom," *ASME Journal of Fluids Engineering*, Vol. 107, Dec. 1985, pp. 495–499.

[9]Wilson, L. O. and Schryer, N. L., "Flow Between a Stationary and a Rotating Disk with Suction," *Journal of Fluid Mechanics*, Vol. 85, 1978, pp. 479–496.

[10]Wilson, L. O., "A New Look at the Burton, Prim, and Slichter Model of Segregation During Crystal Growth from the Melt," *Journal of Crystal Growth*, Vol. 44, 1978, pp. 371–376.

[11]Wilson, L. O., "The Effect of Fluctuating Growth Rates on Segregation in Crystals Grown from the Melt," *Journal of Crystal Growth*, Vol. 48, 1980, pp. 435–450.

[12]Ostrach, S., "Fluid Mechanics in Crystal Growth—The 1982 Freeman Scholar Lecture," *ASME Journal of Fluids Engineering*, Vol. 105, 1983, pp. 5–20.

[13]Langlois, W. E., "Effect of the Buoyancy Parameter on Czochralski Bulk Flow in Garnet Growth," *Journal of Crystal Growth*, Vol. 46, 1979, pp. 743–746.

[14]Ostrach, S., "Low-Gravity Fluid Flows," *Annual Review of Fluid Mechanics*, Vol. 14, 1982, pp. 313–345.

[15]Hyun, J. M. and Kim, J. W., "Flow Driven by a Shrouded Spinning Disk with Axial Suction and Radial Inflow," *Fluid Dynamics Research*, Vol. 2, 1987, pp. 175–182.

[16]Kamotani, Y. and Ostrach, S., "Design of a Thermocapillary Flow Experiment in Reduced Gravity," *Journal of Thermophysics*, Vol. 1, No. 1, 1987, pp. 83–89.

[17]Pedlosky, J., "Geophysical Fluid Dynamics," *Geophysical Fluid Dynamics Lecture Notes*, American Mathematical Society, 1971, pp. 1–60.

[18]Hyun, J. M., Leslie, F., Fowlis, W. W., and Warn-Varnas, A., "Numerical Solutions for Spin-Up from Rest in a Cylinder," *Journal of Fluid Mechanics*, Vol. 127, 1983, pp. 263–281.

[19]Warn-Varnas, A., Fowlis, W. W., Piacsek, S., and Lee, S. M., "Numerical Solutions and Laser-Doppler Measurements of Spin-Up," *Journal of Fluid Mechanics*, Vol. 85, 1978, pp. 609–639.

[20]Batchelor, G. K., "Note on a Class of Solutions of the Navier-Stokes Equations Representing Steady Rotationally-Symmetric Flow," *Quarterly Journal of Mechanics and Applied Mathematics*, Vol. 4, 1951, pp. 29–41.

[21]Allen, J. S., "Upwelling of a Stratified Fluid in a Rotating Annulus: Steady State. Part 2. Numerical Solutions," *Journal of Fluid Mechanics*, Vol. 59, 1973, pp. 337–368.